

# An integrative dynamical perspective for graph theory and the study of complex networks

Gorka Zamora-López<sup>1,2, a)</sup> and Matthieu Gilson<sup>3</sup>

<sup>1)</sup> *Center for Brain and Cognition, Pompeu Fabra University, Barcelona, Spain.*

<sup>2)</sup> *Department of Information and Communication Technologies, Pompeu Fabra University, Barcelona, Spain.*

<sup>3)</sup> *Institut des Neurosciences des Systemes, INSERM-AMU, Marseille, France.*

Built upon the shoulders of graph theory, the field of complex networks has become a central tool for studying a wide variety of real systems across many fields of research. Represented as a graph, all those systems can be studied using the same analysis methods allowing for their comparison. In this perspective we challenge the extended idea of graph theory as being a data-driven analysis tool. Instead we show that classical graph metrics (e.g., degree, matching index, clustering coefficient and geodesic distance) arise from a common hidden generative propagation model: the discrete cascade. From this model-based, dynamical perspective, graph metrics are no longer regarded as combinatorial properties of the graph but as spatio-temporal characteristic of the network, unfolded at different temporal scales. Once we acknowledge graph analysis as a dynamical, model-based analysis tool, we are free to replace the original discrete cascade by other propagation models and to derive new network metrics. Explicitly and transparently, opening the opportunity to design personalized network analyses for different classes of real networks by choosing generative models that fulfil the minimal constraints of the empirical systems under study. Thus balancing between simplicity and interpretability of results.

Keywords: Complex networks; graph theory; network analysis; model-based methods; propagation dynamics; random walkers

---

<sup>a)</sup> Electronic mail: gorka@Zamora-Lopez.xyz

## I. INTRODUCTION

**B**uilt upon the shoulders of graph theory, the field of complex networks has become a central tool for studying a wide variety of real systems across many fields of research, e.g. sociology<sup>1</sup>, epidemiology<sup>2</sup>, neuroscience<sup>3-6</sup>, biology<sup>7,8</sup>, chemistry<sup>9,10</sup> and telecommunications<sup>11</sup>. The success of graph theory to permeate over such a variety of domains lies on its simplified representation. In the eyes of graph theory, a system of interacting elements is reduced to nodes and edges. A graph is an abstract manner to describe empirical systems which provides them with a “form” that is mathematically tractable, thus allowing to uncover their hidden architecture and to investigate how this architecture is related to—or affected by—the functions of the real system.

Despite its immense success, the simplicity of graph analysis is at the same time its major limitation. The process of reducing a real system into a graph requires to discard much of the information needed to understand the system. As beneficial as it is to count with a simplified representation and having a common toolbox for all networks, the final step of the analysis is to translate back the outcomes of the graph metrics into interpretations that make sense in the context of the real system. This step—from metrics to interpretation—is prone to personal creativity due to the large simplifications made in first place.

Graph theory is for binary networks by definition: the only relevant information about the interactions is whether a link exist between two nodes or not. However, the connections of empirical systems usually carry weighted links that graph analysis is not suited to deal with. On the one hand, the combinatorial nature of graph theory cannot treat continuous variables representing link weights. On the other hand, the link weights of empirical networks are not just numerical values; they represent physical or statistical quantities. Weighted graph metrics have often been defined by starting from the equations for a binary metric and directly replacing the binary entries by weighted ones. By doing so, we risk ignoring the physical magnitudes of those weights. These limitations underline the need to establish more flexible network analysis tools that are better suited for the variety of real complex systems studied, allowing for their characterization and individual interpretation.

Plenty of work has been devoted to study the bidirectional relation between network structure and the dynamics manifesting on networks<sup>12-15</sup>. Many works have attempted to uncover how specific network features (e.g., the presence of hubs or degree-degree correlations) affect the collective dynamics on a network. Other efforts aimed at employing dynamical processes to reveal the organization of a network and its features by observing the behaviour of diffusion, propagation or routing processes in the network<sup>16-20</sup>. In this perspective we revisit those efforts and we go a step forward by showing that

the relation between graphs and dynamics is not only a matter of practical interest but that a foundational correspondence exists between the two. We expose that graph analysis can be reformulated from the perspective of dynamical systems by showing that popular graph metrics arise from a simple but common generative dynamical model: a cascade of discrete agents, which is also discrete in time and rapidly diverges. From this dynamical perspective, graph metrics are no longer regarded as combinatorial properties of the graph but as spatio-temporal characteristic of the network, unfolded at different temporal scales after unit perturbations are applied at the nodes.

We believe that exposing this dynamical viewpoint of graph metrics is relevant for various reasons and opens new opportunities for the study of complex networks in a more pragmatic manner. First, it allows to frame the ecosystem of dynamical approaches to characterise networks into perspective, providing a common umbrella to encompass them. Second, it reveals that graph analysis is model-based rather than a data-driven analysis toolbox. Hence, every time we employ graph metrics we are implicitly assuming that a discrete cascade—together with its assumptions and constraints—is the *right* model to describe a real network. Third, it shows that some of the limitations of graph theory are not necessarily of combinatorial nature, but are associated with the constraints of the discrete cascade behind graph metrics. And last, once we acknowledge graph analysis as a model-based analysis tool, there is no need to get married with a unique model, assumed to be meaningful for all cases. Instead, we are free to replace the original discrete cascade by other propagation models and to derive new network metrics in a similar fashion. Explicitly and transparently. This flexibility will allow to define network metrics in which link weights are built-in, and it provides the opportunity to calibrate network analyses by choosing generative models that respect the minimal constraints of the particular real system under study. Thus balancing between simplicity and interpretability of results.

The paper is organised as follows. Section II describes the dynamical formulation of graph metrics as emerging from a discrete cascading process. Section III illustrates how networks can exhibit different faces depending on the dynamical process employed to observe them, indicating the need for a generalization of network analysis in which the underlying propagation model is replaceable and explicit. Section IV illustrates some benefits of a dynamical approach to network analysis such as a generalised distance metric and network comparison. Last, Section V provides an overview of past efforts to characterize graphs using dynamics and clarifies how those attempts fall together into a common umbrella of the perturbative formalization here proposed.

## II. A DYNAMICAL REPRESENTATION OF GRAPH ANALYSIS

Graphs are typically encoded either as adjacency matrices or adjacency lists. For a graph  $G$  made of  $n$  nodes its adjacency matrix  $A$  is a matrix of shape  $n \times n$  with entries  $a_{ij} = 1$  if there is a link connecting nodes  $i$  and  $j$ , or  $a_{ij} = 0$  otherwise. Adjacency lists, on the other hand, are the sets of edges  $E(G) = \{(i, j)\}$  for those nodes  $i$  and  $j$  that are connected by a link. For graph theory, all relevant information about a network is encoded in  $A$  or  $E(G)$ . However, neither the adjacency matrix nor the adjacency list explain the underlying architecture of the graph. For that, graph analysis consists of applying a variety of metrics to extract information that allows to clarify the “form” of a graph. Uncovering the architecture of a network is like building a puzzle because no single graph metric conveys all necessary information we need to fully understand the network. Each metric provides us with a useful but incomplete piece of information about the architecture of the network, and only by integrating several pieces together we can understand how it is organised.

Although graph theory is a branch of combinatorial mathematics, algorithmically speaking, graph metrics are rarely evaluated employing combinatorial tools. Instead, most graph metrics are computed by exploring the graph via depth-first-search (DFS) or breath-first-search (BFS) algorithms and applying different rules along the process. From a dynamical point of view DFS and BFS represent two very different propagation processes. Depth-first search corresponds to a conservative dynamical process in which a single agent navigates through the entire graph. The agent moves from one node to another along a link connecting them. This is similar to processes of random walkers since at all time steps there is a unique agent on the network—the one initially seeded. The difference with random walkers is that in a DFS the agent navigates through the network in a prestablished order while a random walker randomly chooses which neighbour visits at the following time step.

On the contrary, BFS represents a non-conservative cascading process because for every particle sitting on a node at time  $t$ , the process gives rise to one new particle per neighbour at the following iteration  $t + 1$ . That is, in a BFS type of propagation, agents are not passively transported from one node to another through links. Instead, the outgoing links of a node actively create new particles every time step. Therefore, the number of particles in the network rapidly grows over time. Such a cascade is illustrated in Figure 1 for a single particle (a tennis ball) initially seeded at node  $i = 7$ . This node has a single neighbor and thus at time  $t = 1$  node  $i = 6$  receives one ball. At the next iteration, however, node  $i = 6$  has four neighbors and thus each neighbor receives one ball. At time  $t = 3$  nodes  $i = 6$  and  $i = 4$  receive more than one ball. Therefore, at time  $t = 4$  these two nodes will give to their neighbours one new ball, one per

each ball they already had.

Without a queue to remember the nodes visited, the dynamical system that describes the cascade behind BFS is the discrete mapping  $f : \mathbb{N}^n \rightarrow \mathbb{N}^n$  of the form:

$$\mathbf{x}_t = A \mathbf{x}_{t-1}, \quad (1)$$

where  $\mathbf{x}_t$  is the state (vertical) vector of the  $n$  nodes. The values  $x_{i,t} \in \mathbb{N}$  represent the number of particles found in node  $i$  at time  $t$ . In principle, the BFS starts with a single particle at a selected node, e.g., choosing  $i = 2$  as the root vertex for a network of  $n = 5$  nodes, the process would start from the initial conditions  $\mathbf{x}_0^T = (0, 1, 0, 0, 0)$ . Let us initially seed one particle at every node such that  $\mathbf{x}_0 = \mathbf{1}$  with  $x_{i,0} = 1$  for all  $i$ . The solutions of the discrete cascade at times  $t > 0$  are obtained recursively from Eq. (1), such that:

$$\begin{aligned} \mathbf{x}_1 &= A \mathbf{x}_0 = A \mathbf{1}, \\ \mathbf{x}_2 &= A \mathbf{x}_1 = A(A \mathbf{x}_0) = A^2 \mathbf{x}_0 = A^2 \mathbf{1}, \\ \mathbf{x}_3 &= A \mathbf{x}_2 = A(A(A \mathbf{x}_0)) = A^3 \mathbf{x}_0 = A^3 \mathbf{1} \\ &\vdots \\ \mathbf{x}_t &= A^t \mathbf{x}_0 = A^t \mathbf{1}. \end{aligned} \quad (2)$$

The recursive nature of the process implies that the solution at any time  $t$  is trivially determined by two quantities: the initial conditions  $\mathbf{x}_0 = \mathbf{1}$  and the powers of the adjacency matrix  $A^t$  acting as the propagators (also known as the *Green function*) of the process over time. Strictly speaking, the values  $(A^t)_{ji}$  are the number of particles found in node  $j$  at time  $t$ , due to the single particle initially seeded at node  $i$ . More generically, the values  $(A^t)_{ij}$  can be interpreted in two complementary manners. On the one hand, as the *influence* that an initial unit perturbation at node  $i$  exerts on node  $j$  over time, or on the other hand, as the *temporal response* of node  $j$  to a unit perturbation applied on  $i$  at time  $t = 0$ . It is important to note that this conditional pair-wise response encompasses all network effects from  $i$  to  $j$  acting at different time scales along all (non-Hamiltonian) paths of different lengths.

At this point, a connection can be drawn between graph theory—as a combinatorial subject—and the dynamical nature behind the calculation of graph metrics. From graph theory it is well known that the powers of the adjacency matrix  $A^l$  encode the number of non-Hamiltonian paths of length  $l$  between two nodes, or the number of cycles of length  $l$  in which a node participates. For example, the entry  $(A^3)_{ij}$  represents the number of all (non-Hamiltonian) paths of length  $l = 3$  starting at node  $i$  that reach node  $j$ . If  $i = j$ , then  $(A^3)_{ii}$  is the number of triangles in which  $i$  participates. From a purely combinatorial point of view counting and identifying all possible paths of a given length in a network is a difficult problem to tackle since the number of branches and choices rapidly grow with the length. However, from the dynamical point of view it is a rather trivial exercise.

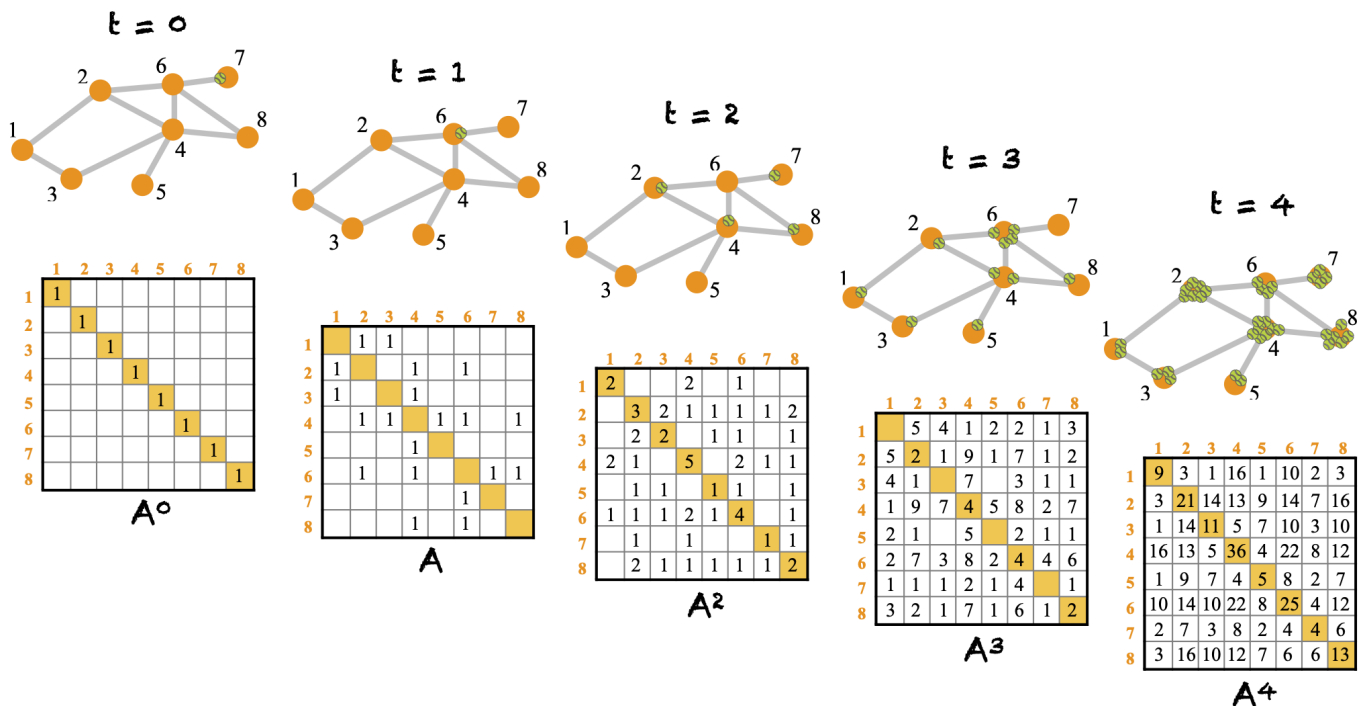


FIG. 1. **Representation of graph metrics as a discrete cascade** From the perspective of graph theory, the powers of the adjacency matrix  $A^t$  represent the number of non-Hamiltonian paths between two nodes. However, from a dynamical perspective,  $A^t$  are the number of particles found in a node  $j$  at any given time  $t$  due to a single particle initially seeded in node  $i$  at time  $t = 0$ . This is true when the propagation of the agents or particles is governed by a discrete cascade.

As the derivations above reveal, the combinatorial problem is equivalent to study the propagation of a discrete cascade in the network—one of the simplest dynamical models that can be defined. Our aim here is to show that more than an exceptional coincidence, the dynamical equivalence and interpretation is common for graph metrics, in particular for the most popular and informative ones.

To do so, we realise that all the relevant information needed to characterise the network and to define graph metrics is unfolded—via the generative dynamics—from the adjacency matrix  $A$  onto the response matrices  $\mathcal{R} = \{A^0, A^1, A^2, A^3, \dots, A^t\}$ . In Appendix we show how several graph metrics (node degree, matching index, clustering coefficient and geodesic distance) are in fact derived from the set of response matrices  $\mathcal{R}$ . From these derivations we learn two conclusions. First, from this dynamical perspective, graph metrics are no longer regarded as combinatorial attributes of the graph but they correspond to spatio-temporal properties of the network's response to external (unit) perturbations. Second, although the discrete cascade is a system that rapidly diverges, graph metrics are not affected by this because they only represent the properties of the network responses at very short time scales. As shown in Appendix 1, both the degree and the matching index are network attributes expressed at time  $t = 2$  the clustering coefficient is a network feature at time  $t = 3$ . The geodesic distance is the

only one that may result from the cascading process at longer time scales (up to  $t = n - 1$  if the graph is connected). But for the common small-world real networks, it spans only for times  $t \ll n$ .

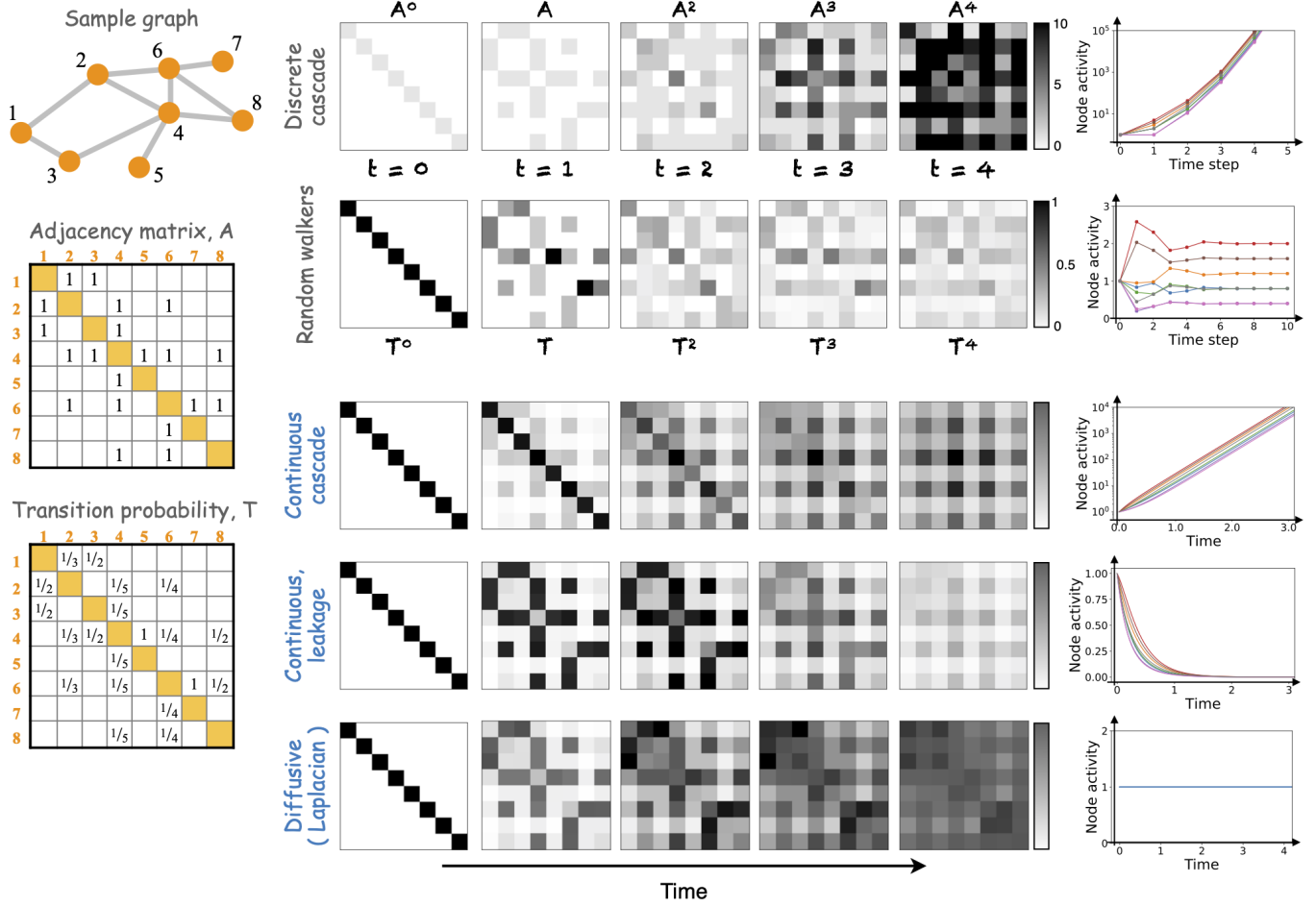
### III. PROPAGATION MODEL SELECTION FOR PERSONALIZED NETWORK ANALYSIS

The derivations in the previous section and in Appendix 1 allowed us to draw a foundational relation between graph theory and network dynamics by showing that typical graph metrics can be derived from a common generative model—the discrete cascade in Eq. (1)—and, therefore, those metrics can be interpreted as spatio-temporal properties of the network responses to initial unit perturbations. Although defining and deriving the graph metrics from the set of response matrices  $\mathcal{R}_t = \{A^0, A^1, A^2, A^3, \dots, A^t\}$  may seem a complication, this dynamical representation implies two relevant consequences. On the one hand, it reveals that every time we perform graph analysis, we are assuming that the discrete cascade is the appropriate dynamical model to describe the real network under study. Given the wide variety of empirical systems studied with graph analysis, it is unrealistic to assume that one propagation model serves to characterise and interpret all real networks. On the other hand, it opens the door to alleviate this problem by

### A Generative propagation models

Cascade	Random walkers	Cascade	Leakage	Diffusive ( Laplacian )
$\mathbf{x}_t = A \mathbf{x}_{t-1}$	$\mathbf{x}_t = T \mathbf{x}_{t-1}$	$\dot{\mathbf{x}} = A \mathbf{x}$	$\dot{\mathbf{x}} = -\frac{1}{\tau} \mathbf{x} + A \mathbf{x}$	$\dot{\mathbf{x}} = -D \mathbf{x} + A \mathbf{x} = L \mathbf{x}$
Discrete, divergent non-conservative	Discrete, convergent conservative	Continuous, divergent non-conservative	Continuous, convergent non-conservative	Continuous, convergent conservative
$\mathcal{R}_t = \{A^0, A^1, A^2, \dots, A^t\}$	$\mathcal{R}_t = \{A^0, T^1, T^2, \dots, T^t\}$	$\mathcal{R}(t) = e^{At}$	$\mathcal{R}(t) = \left( e^{Jt} - e^{J^0 t} \right)$	$\mathcal{R}(t) = \left( e^{Lt} - e^{L^0 t} \right)$

### B Model replacement



### C Network responses

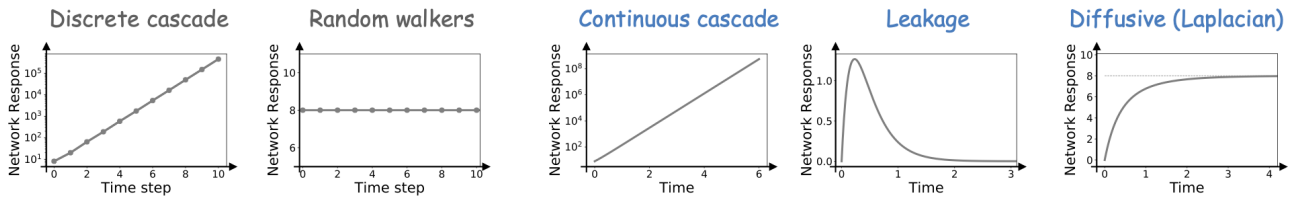


FIG. 2. **Characterizing networks under the light of different dynamical processes.** **A** Equations, basic conditions and temporal response matrices of five simple propagation models, two discrete (gray) and three continuous (blue). **B** Illustration of model replacement to derive network metrics applied to a sample graph of eight nodes. For each model the response matrices at different times are shown (grayscale matrices). The diagonal matrices in all cases represent the initial conditions, consisting of a unit perturbation at each node. In all cases except for the continuous cascade, the color scale of the matrices is adjusted to the same level in each model. Due to the explosive growth of the continuous cascade, matrices are shown for arbitrary colorscales in order to highlight the patterns. Panels on the right hand side show the temporal solutions  $x_i(t)$  for the eight nodes in the graph, highlighting the divergent, conservative or decaying nature of the four models. **C** Network responses  $r(t)$  over time.

developing a family of graph analysis *flavours*. Once we have acknowledged that graph analysis is a model-based data analysis tool, we are free to replace the underlying propagation model and design analyses that are better suited for the individual real networks of interest. We envision that in the future, before performing a network analysis, the user will first identify which are the fundamental constraints of the real system investigated (e.g., is it discrete, or is it a continuous system? Is it conservative, or non-conservative?). Once the fundamental ingredients are clear, the user could select the simplest propagation model that satisfies those conditions and develop a personalised network analysis that is tuned for that real network; or for a domain of real networks.

In the following, we illustrate how such families for personalised graph analyses could be derived, both for discrete and for continuous generative dynamical models. The goal is, as mentioned above, to identify the network responses  $\mathcal{R}$  to an initial unit perturbation for different models, and then to extract the information about the network from  $\mathcal{R}$ .

A popular propagation model often employed to explore networks is the random walker. The random walk is, as the cascade in Eq. (1), a discrete dynamical model both in variable and in time. The main difference with the cascade is that the random walker represents a conservative system in which one agent, the walker, perpetually navigates through the network. That is, for every walker initially seeded, there is one, and only one walker in the network at all times. On the contrary, for the discrete cascade, at every time-step, every particle in node  $i$  results in  $k_i$  new particles. Given the adjacency matrix  $A$ , the transition probability matrix  $T$  is defined by normalising the columns by their total degree. Hence, entries  $T_{ij}$  represent the probability that a walker located at node  $i$  at time  $t$  has to visit one of the  $k_i$  neighbours at time  $t + 1$ . Formally, the random walker is a mapping  $f : \mathbb{R}^n \rightarrow \mathbb{R}^n$  of the form:

$$\mathbf{x}_t = T \mathbf{x}_{t-1}, \quad (3)$$

where the elements  $x_i(t)$  represent the expected number of walkers on node  $i$  at time  $t$ . As for the discrete cascade, the solution of Eq. (3) is iterative. Given initial conditions  $\mathbf{x}_0$ , the solution is for any time  $t > 0$  is  $\mathbf{x}_t = T^t \mathbf{x}_0$ . If we allow one walker to start from each node,  $x_i(0) = 1$ , the resulting response matrices are  $\mathcal{R} = \{T^0, T^1, T^2, T^3, \dots, T^t\}$ .

Figure 2 shows the response matrices of the same sample graph for five distinct generative models, two discrete and three continuous). Comparing the results for the discrete cascade and the random walkers, it is seen that the two models give rise to different patterns of pair-wise responses. At the first iteration  $t = 1$  the  $\mathcal{R}_1$  matrices of both models display a similar pattern that reflects direct connections. But in the subsequent iterations the response matrices begin to differ between the two models. This shows that model selection matters for the analysis

of networks, as each propagation model highlights different aspects of the underlying graph.

A major difference between the two models is that the cascade is a divergent process while the random walk is a conservative propagation. The panels on the right display the solutions  $x_{i,t}$  for the eight nodes over time. As seen, the number of agents on each node rapidly grows for the cascade while the expected number of walkers on a node stabilises after a short transient. The divergent or conservative nature of the two models is also reflected in the response matrices. We define the network response  $r(t)$  as the sum of all pair-wise responses at each time step,  $r(t) = \sum_{i,j=1}^n \mathcal{R}_{ij}(t)$ . Figure 2C shows the evolution of the network responses for the five models. For the discrete cascade, its network response rapidly grows because at each iteration, every particle gives rise to  $k_i$  new particles. However, for the random walkers,  $r(t) = 8$  at all times because it is a conservative system and we initially seeded eight walkers, one per node.

### Continuous propagation models

The extension of Eq. (1) into the continuous realm is given by the following differential equation:

$$\dot{\mathbf{x}}(t) = A \mathbf{x}(t), \quad (4)$$

where  $\mathbf{x}^T(t) = [x_1(t), x_2(t), \dots, x_n(t)]$  is the real-valued state vector of the  $n$  variables and  $A$  is a real-valued, positive connectivity matrix not restricted to binary. Given initial conditions  $\mathbf{x}_0$ , the solution of this system is:

$$\mathbf{x}(t) = e^{At} \mathbf{x}_0. \quad (5)$$

In this case, the propagator—or Green function—of the network is the function

$$\mathcal{R}(t) = e^{At} \quad (6)$$

instead of the set of power matrices seen for the discrete models. At every time  $t'$ ,  $\mathcal{R}(t')$  is a matrix of shape  $n \times n$  whose elements  $\mathcal{R}_{ij}(t') = \left(e^{At'}\right)_{ij}$  represent the temporal evolution of the response of node  $j$  at times  $t' > 0$  to a unit perturbation applied in node  $i$  at time  $t = 0$ . Or, equivalently,  $\mathcal{R}_{ij}(t)$  is the influence that node  $i$  exerts on  $j$  over time. As for the discrete cascade,  $\mathcal{R}(t)$  encompasses this influence along all possible paths, of all lengths converging into  $j$  at different times. With the difference that now the connectivity  $A$  could be weighted and, in that case,  $\mathcal{R}_{ij}(t)$  would enclose the influence over all weighted routes. Hence, the response is typically larger between nodes directly connected by strong links, and smaller between nodes connected by weaker links, or not directly connected and relying on indirect paths.

In Fig. 2B, the evolution of the response matrices  $\mathcal{R}(t) = e^{At}$  is shown at various temporal snapshots for the small sample graph. As seen in the first snapshot,

short after the perturbation the responses are governed by the direct connections and  $\mathcal{R}(t)$  resembles the adjacency matrix  $A$ . But as time passes and the influence between nodes expands to longer paths, the patterns  $\mathcal{R}(t)$  change and dissociate from  $A$ . The continuous cascade is also a divergent system and the solutions (node activity)  $x_i(t)$  grow exponentially as depicted in the panel at the right. Same fate goes for the network response  $r(t)$ , in Fig. 2C.

Divergent dynamics are rarely representative of empirical systems. A strategy to avoid divergence in Eq. (4) is to include a dissipative term as follows:

$$\dot{\mathbf{x}}(t) = -\frac{1}{\tau}\mathbf{x}(t) + A\mathbf{x}(t). \quad (7)$$

The term  $-\mathbf{x}/\tau$  implies that part of the flow passing through a node will leak, compensating for the exponential growth of the cascading term  $A\mathbf{x}$ . The relaxation time-constant  $\tau$  controls for the ratio of the leakage: the shorter the  $\tau$  the faster the nodes leak. When  $\tau = 0$  all the flow is lost through the nodes and nothing will flow from one node to another. Given that  $\lambda_{max}$  is the largest eigenvalue of the (weighted) connectivity  $A$ , the leakage can only compensate the cascading term as long as  $0 \leq \tau < 1/\lambda_{max}$ . When  $\tau \geq 1/\lambda_{max}$  the exponential growth dominates and the system becomes divergent.

In this case, we define the network response to an initial unit perturbation  $\mathbf{x}_0 = \mathbf{1}$  as<sup>20,21</sup>:

$$\mathcal{R}(t) = \left( e^{Jt} - e^{J^0 t} \right) \quad (8)$$

where  $J = -\delta_{ij}/\tau + A_{ij}$  is the Jacobian matrix of System (7) and  $J^0 = -\mathbf{x}/\tau$  is for the leakage term. In Eq. (8),  $J^0$  is regressed out because we are only interested in the responses of the nodes due to the pair-wise interactions.  $J^0$  only represents the passive leakage of the initial perturbation on a node through itself. In this case, the direct connections are more relevant than previously found for the cascade. The patterns of the response matrices at the initial times are dominated by the shape of the connectivity matrix  $A$ , see Fig. 2B. Only at the longer times, the patterns displayed by  $\mathcal{R}(t)$  change and dissociate from  $A$ . As expected, the solutions  $x_i(t)$  for the individual nodes decay and relax to zero, right panel of Fig. 2B. However, the network response  $r(t)$  undergoes a transient peak at the shorter times to later decay and relax to zero, Fig. 2C. and an initial phase of growth at early times but peaks and decays after a tran follow the shape of the connectivity  $A$  at the initial times temporal evolution of  $\mathcal{R}(t)$  matrices in this case is shown in represent the temporal response of node  $j$  at times  $t > 0$  to an initial perturbation on node  $i$ . For adequate values  $\tau$ , all pair-wise responses vanish after an initial transient. Response matrices to an initial unit perturbation for this case on the sample network are shown in Fig. 2B together with the decaying individual solutions  $x_i(t)$  of Eq. (7) for each node. The transient behaviour of the total network response  $r(t)$  is shown in Fig. 2C.

## Diffusive coupling and the Laplacian matrix

The two continuous models described so far are non-conservative because the coupling  $i \rightarrow j$  is mediated by passing the state  $x_i$  of node  $i$  to the target node  $j$ . Thus, the total response of  $j$  is the sum  $\sum_{i=1}^n A_{ij}x_i$  of the states of its neighbours. However, the interaction between nodes in many systems is mediated by the difference  $(x_j - x_i)$  between the nodes, as is for example the case in the Kuramoto model. In the Kuramoto, the strength of the interaction between two oscillators is proportional to their phase differences:  $\dot{\theta}_i \propto \sum_{j=1}^n \sin(\theta_j - \theta_i)$ . This type of coupling by the differences is usually termed as *diffusive coupling* and is characteristic of conservative dynamical systems because it guides nodes towards the mean-field.

The simplest linear propagation model based on diffusive coupling can be written by:

$$\dot{x}_i = \sum_{j=1}^n A_{ji}(x_j - x_i). \quad (9)$$

Since the sum only affects the  $j$  index, we have that  $\dot{x}_i = \sum_{j=1}^n A_{ji}x_j - \sum_{j=1}^n A_{ji}x_i$ . If  $A$  is the binary and symmetric adjacency matrix, then  $\sum_{j=1}^n A_{ji} = k_i$  the degree of node  $i$ . Thus, the system can be re-written as:

$$\dot{x}_i = -k_i x_i + \sum_{j=1}^n A_{ji}x_j. \quad (10)$$

Defining  $D$  as the diagonal matrix with entries  $D_{ii} = k_i$ , we express the system in matrix form:

$$\dot{\mathbf{x}} = -D\mathbf{x} + A\mathbf{x} = L\mathbf{x}, \quad (11)$$

where  $L = -D + A$  is usually known as the *Laplacian matrix*. Comparing Eqs. (7) and (10), it shows that this conservative system could be regarded as a special case of the leaky-cascade system only that here the time-constants of the nodes are individually tuned such that  $\tau_i = \frac{1}{k_i}$ . This tuning balances the input and the leakage ratios at every node. All the input that arrives to a node is leaked, thus setting a zero net flow at all time points.

The solution of Eq. (11) with initial conditions  $\mathbf{x}_0 = \mathbf{1}$  is  $\mathbf{x}(t) = e^{Lt} \mathbf{x}_0$ . Following the rationale for the definition of the response function for the leaky cascade, we define:

$$\mathcal{R}(t) = \left( e^{Lt} - e^{L^0 t} \right) \quad (12)$$

where  $L^0 = -D\mathbf{x}$  is the leakage term. The temporal evolution of  $\mathcal{R}(t)$  is depicted in Fig. 2B (bottom panels). Again, the initial moments post-stimulation  $\mathcal{R}(t)$  seems governed by the direct connections although at subsequent times the patterns change. In particular, it can be seen that the connections of the most connected node rapidly start to loose relevance, as compared to the responses of the leaky-cascade in which the hub is reinforced at early times. Given the zero net flow

through the nodes, their solution is constant  $\mathbf{x}(t) = \mathbf{1}$  for all  $t$ , right panel at the bottom of Fig. 2B. For the same reason, the network responses  $r(t) = 8$  as the sum of the unit contribution of the eight nodes.

Summarizing, in this section we have illustrated how to define the network responses  $\mathcal{R}$  to a unit perturbation for five simple propagation models. Two discrete and three continuous. Two of them represent conservative dynamics and three are non-conservative. This five models could serve as the underlying generative dynamics to perform model-based network analysis, suited for different classes of real systems. The goal, as stated above, is to extract information about the network by defining metrics from the spatio-temporal responses  $\mathcal{R}$ . Importantly, the results depicted in Fig. 2B expose that one network, the small sample graph depicted, can display different faces depending on the dynamical model employed to “observe” it. Each dynamical model expresses the various features of the network in a different manner. For example, here the leaky cascade seems to expose the connections of the hub robustly (node  $i = 4$  in the sample graph) while the approach based on the diffusive coupling—the Laplacian matrix—tones down the links of the hub and reinforces instead the links between peripheral nodes (e.g., links 1–2 and 1–3 of the sample graph).

#### IV. EXAMPLES AND APPLICATION

The core idea of this perspective is that all the information needed to characterise a network is encoded in the spatio-temporal responses to a unit perturbation,  $\mathcal{R}$ , which differs depending on the generative model of choice. Once  $\mathcal{R}$  is defined for a given model, the challenge is then to derive network metrics from  $\mathcal{R}$  to describe the network, in line with the finding that classical graph metrics originate from the power matrices  $\mathcal{R}_t = A^t$  associated to the discrete cascade. While detailed derivation of measures shall be regarded as a future endeavour, we now provide examples to illustrate that the dynamical approach to network analysis here proposed can serve to overcome some of the limitations of classical graph analysis. We first explain how to derive a more general definition of distance between nodes for the continuous case, and then we deal with the problem of network comparison. For these proofs of concept we will restrict to the continuous propagation with leakage in Eq. (7) and its response function, Eq. (8).

##### Graph distance as response times

In graphs, the (geodesic) distance between two nodes  $i$  and  $j$  is quantified as the smallest number of links that an agent needs to traverse, hopping through links, to go from node  $i$  to  $j$ , Fig. 3A. However, this concept is only

valid for the case of unweighted, binary graphs and discrete agents or particles navigating in the network. If the edges of a graph are weighted, or the system cannot be represented by discrete particles, then the idea of an agent ‘hopping’ through links is incompatible and an alternative definition of distance is required. In Appendix 1, we show that from the dynamical perspective here introduced, the graph distance between two nodes corresponds to the time step  $t$  at which a discrete cascade initiated at node  $i$  arrives for the first time in node  $j$ . This redefinition of distance in terms of time allows for a more flexible application.

Consider the leaky-cascade in Eq. (7). The pair-wise responses  $R_{ij}(t)$  due to an initial perturbation at node  $i$ , undergo a transient growth followed by a decay dominated by the leakage term, as depicted in Fig. 3B. In this scenario, we define the distance from node  $i$  to  $j$  as the time required for the response of node  $j$  to an initial perturbation on  $i$  to reach its peak. We demonstrate this on three undirected graphs (random, scale-free-like and a ring lattice) of  $n = 100$  and density  $\rho = 0.1$ . The scale-free-like network was generated for  $\gamma = 2.5$ . The adjacency matrices, the graph distance  $D_{ij}^g$  and the time-to-peak distance  $D_{ij}^{ttp}$  matrices for the three graphs are shown in Fig. 3C. Visually,  $D_{ij}^g$  and  $D_{ij}^{ttp}$  look very much alike, indicating that in this unweighted case measuring time-to-peak or the classical graph distance are qualitatively equivalent. Quantitatively, the agreement is not exact but very similar, Figure 3D. While graph distance is a discrete quantity, time-to-peak is continuous. Thus there is some level of degeneracy in the time-to-peak values taken by all the pairs at the same graph distance. Although this variation is small and a reasonable linear correlation is found between the geodesic distance and the time-to-peak distance.

It shall be noted that in the particular case of the leaky cascade, the response dynamics depends on the intrinsic relaxation time-constant  $\tau$  governing the rate of the leakage. For the examples in Fig. 3 the  $\tau$  were independently chosen for the three networks such that  $\tau = 0.4\tau_{max}$  where  $\tau_{max} = \frac{1}{\lambda_{max}}$  with  $\lambda_{max}$  being the largest eigenvalue of each network. The value of  $\tau$  can alter the linear relation between  $D_{ij}^g$  and  $D_{ij}^{ttp}$  with wider degeneracy and ultimately saturating when  $\tau$  is close to  $\tau_{max}$ . The larger the  $\tau$  the slower is the leakage bringing the system towards the transition from convergent to divergent as the leakage can no longer balance the flow generated by the connectivity.

##### Comparing networks with each other

The outcome of graph metrics is influenced by the size  $n$  and the density  $\rho$  (or number of links  $m$ ) of a network. This dependence difficults the comparison between networks. Imagine we study two graphs  $G_1$  and  $G_2$  of same size  $n_1 = n_2$  but one is denser than the other, say  $\rho_1 = 0.01$  and  $\rho_2 = 0.06$ . If we obtained average



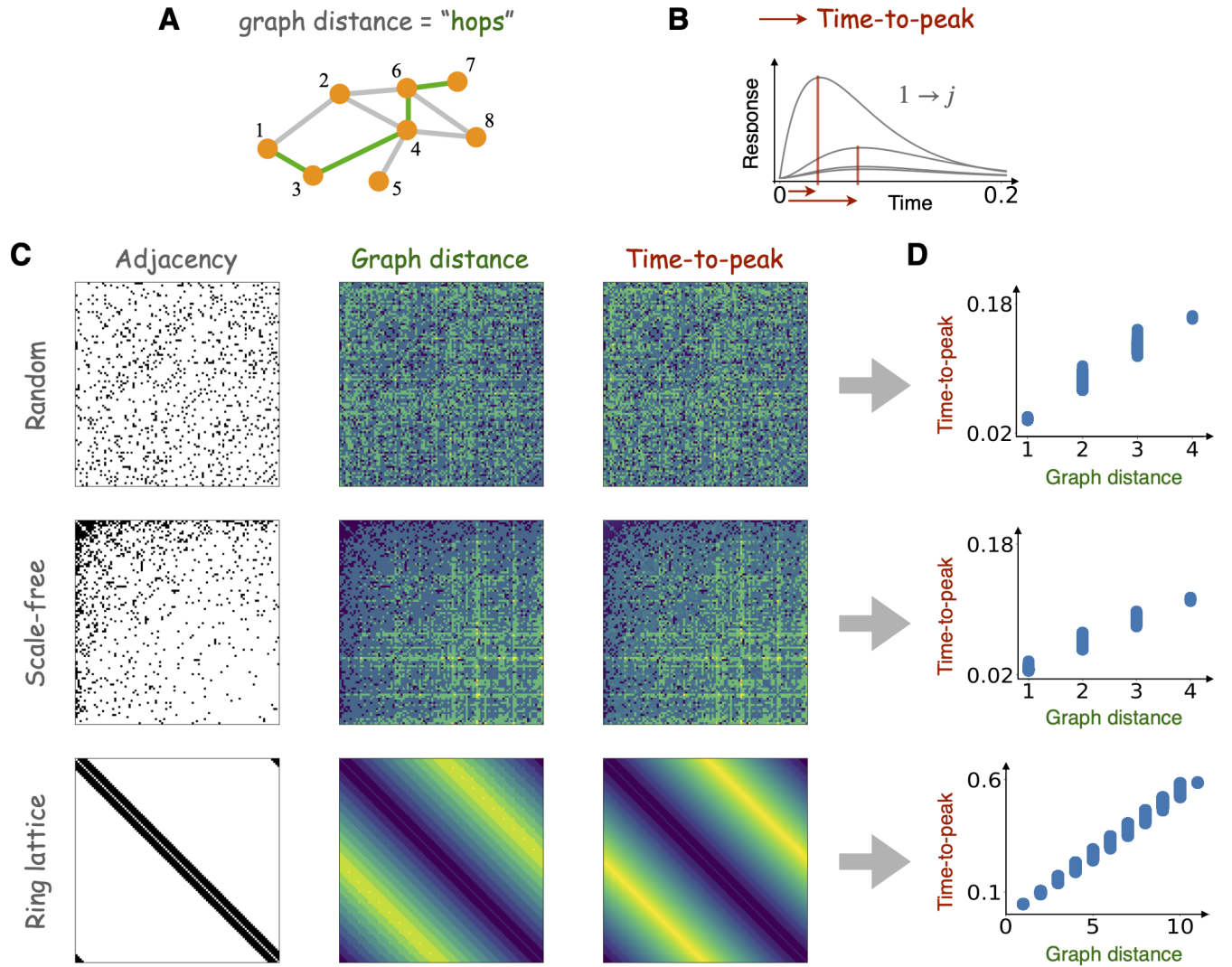


**FIG. 3. Redefinition of distance in networks based on response times** **A** In graphs, the distance between two nodes  $i$  and  $j$  is defined as the number of links needed to traverse in order to travel from one node to another. **B** Under the dynamical perspective here proposed, the distance can be redefined in terms of the time needed for a perturbation at  $i$  to take effect on  $j$ . This could be quantified in different manners, e.g., the time it takes the response to reach the peak. **C** and **D**, validation of equivalence between classical graph distance and time-to-peak distance in three sample graphs: a random graph, an scale-free graph and a ring lattice. **C** Adjacency matrices for the three sample graphs and the corresponding pair-wise distance matrices following the two approaches. Qualitatively, both distance matrices look very much the same. **D** Pair-wise comparison of the distance between all pairs of nodes in the three graphs computed either as classical graph distance  $d_{ij}$  or time-to-peak  $d_{ij}^{ttp}$ . The relation is clearly linear—corroborating the equivalence between the two measures—although some degeneracy in the time-to-peak is found across pairs that lie at same graph distance.

pathlengths  $l_1 = 3.5$  and  $l_2 = 2.9$  respectively, the objective evidence is that  $G_2$  is, as a graph, longer than  $G_1$ . However, it is well-known that the pathlength typically decays with graph density. Hence, we may also want to ask whether  $l_2 < l_1$  simply because  $G_2$  is denser than  $G_1$ , or because their internal architectures differ. In order to answer this question we need to regress out the influences of both size and density on the pathlength. Since the specific dependence of a graph metric on size and density is not always known, the typical strategy to deal with

this problem consists in comparing empirical networks to simple graph models (null-models), e.g. random graphs or degree-conserving random graphs, Fig. 4A. For example, we would construct two ensembles of random graphs matching the size and the number of links of the two graphs studied and we would obtain the corresponding ensemble average pathlengths  $l_{r,1}$  and  $l_{r,2}$ . Then, one would typically compare the relative metrics  $l'_1 = l_1 / l_{r,1}$  and  $l'_2 = l_2 / l_{r,2}$  with each other to derive conclusions about which network is shorter.

This typical procedure suffers from some conceptual and interpretative limitations<sup>22</sup>. From the dynamical perspective to network analysis here proposed there is no need to employ null-models for comparing networks. Instead, a simple normalization of the connectivity suffices to align networks of different size and/or density, making them comparable. The largest eigenvalue of a connectivity matrix  $\lambda_{max}$  captures the intrinsic time scale of the evolution of a network, regardless of the dynamical model. Hence, for any two networks, normalising the connectivity matrices by their corresponding  $\lambda_{max}$  such that  $A' = A/\lambda_{max}$ , aligns the time scales of their responses making them directly comparable<sup>23,24</sup> (see Fig. 4B for illustration). The largest eigenvalues of the normalised connectivities  $A'_1$  and  $A'_2$  are the same:  $\lambda'_{max,1} = \lambda'_{max,2} = 1.0$ . It shall be noted that after the normalization the matrices  $A'_1$  and  $A'_2$  are weighted. Standard graph theory cannot deal with these normalised connectivities as it requires adjacency matrices to be binary, with entries 0 or 1. However, for the dynamical approach to network analysis, dealing with such weighted networks is natural.

In Figs. 4C-E we show the results of this normalization on three network models: random graphs (uniform probability), scale-free-like graphs and Watts-Strogatz graphs. For each of the three models we generated four graphs of size  $n = 200$  or  $500$  nodes, and densities  $\rho = 0.06$  or  $0.1$ . We studied the responses  $\mathcal{R}(t)$  of the networks using the leaky continuous cascade as the generative dynamics and following Eq. (8). Within each model, the network responses  $r(t)$  of the four graphs (top panels) follow different amplitudes and characteristic time-scales despite the internal architecture of the networks are equivalent—as they are instances of the same graph model. Next, we normalised the connectivity matrices by their corresponding  $\lambda_{max}$  and recomputed the responses  $\mathcal{R}'(t)$ . As shown (bottom panels), the normalisation aligns the temporal scales of the four networks. The response curves  $r'(t)$  collapse in pairs of different amplitude. The difference in response amplitudes depend only on the network size. A further normalization of the responses  $\mathcal{R}'(t)$  by network size  $n$  would fully align the four curves, however, that would not imply making the networks more comparable. The effect of normalisation by  $\lambda_{max}$  is that the average response per node is the same in all networks. This aligns the internal variances of the network that arise from the internal architecture.

We illustrate this studying the relation between the node-wise responses and the node degrees in the original graph before and after the normalization. The node response  $r_i(t)$  are defined as the temporal response of a node to all the initial perturbations. It is computed as the column or row sums of the response matrices:  $r_i(t) = \sum_{j=1}^n \mathcal{R}_{ij}(t)$ . Then, the total node response  $r_i$  accounts for the accumulated response at the node from the initial time  $t = 0$  and it is calculated as the integral (or area under the curve) over time  $r_i = \int_{t=0}^{\infty} r_i(t) dt$ . A linear relation between the original degrees  $k_i$  of the bi-

nary graph and the node responses  $r_i$  is observed in all the networks. Networks generated out of the same graph model are expected to follow the same degree distribution although the actual values  $k_i$  tend to grow with network size and density. In the comparison to  $r_i$  before the normalisation (top panels), we find the same trend happens for the  $r_i$  values taken by the nodes. Their absolute values grow with  $n$  and  $\rho$  of the underlying original graphs forming separate “clouds” of points in the plots. However, after the adjacency matrices have been normalised (bottom panels), the values for the responses  $r'_i$  of the four networks become aligned, showing that both the  $r_i$  values and their distributions  $p(r_i)$  are now directly comparable across networks.

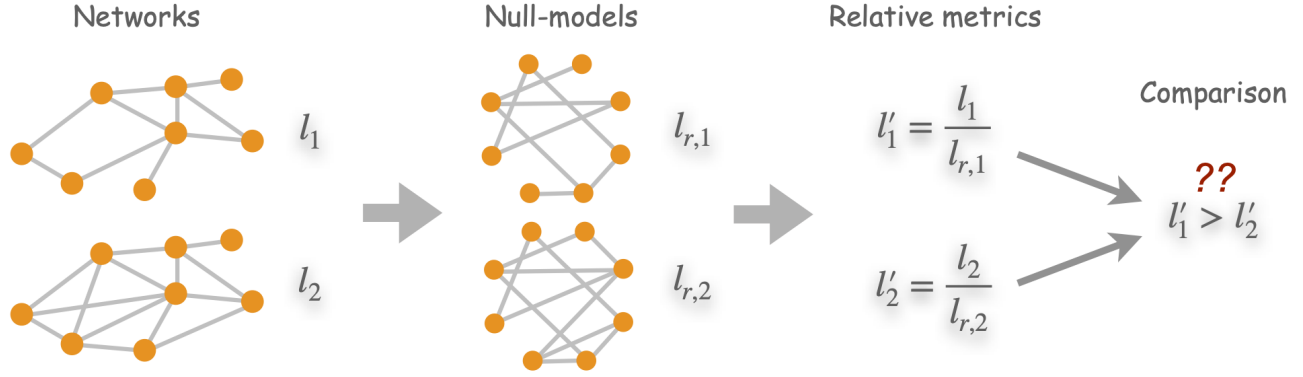
## V. RELATION WITH PAST WORKS

The relation between network structure and function has attracted significant attention in the recent years. More specifically, *function* is usually referred in the literature to imply the behaviour of dynamical phenomena happening on a network. Typically, the study of this relation falls in one of the following three categories: (i) Investigations that aim at uncovering how network architecture or network features (e.g., the degrees of nodes or the presence of motifs) affect the dynamics on a network<sup>12</sup>. (ii) Studies making use of dynamical processes in order to reveal the architecture of the networks or specific network properties, e.g., community identification or defining centrality measures<sup>16,17,19,24–26</sup>. The present article falls in this category. And (iii) studies of network inference aiming at guessing the unknown or incomplete information about the architecture of a network out of empirically observed dynamics<sup>27–29</sup>.

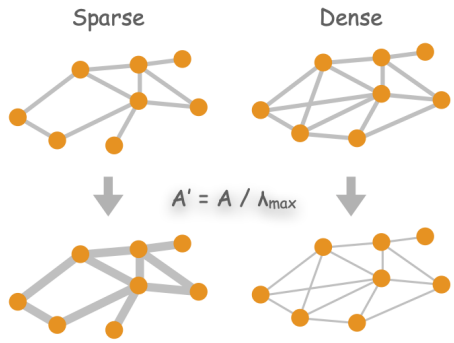
Three types of dynamical approaches are usually investigated on networks. (i) Coupled dynamical systems constructed by placing a dynamical unit at each node which interacts with other nodes according to an underlying connectivity matrix. Examples of such coupled node dynamics could be neurons, oscillators or chaotic attractors. (ii) Propagation, diffusion, spreading or navigation dynamics. This class comprises a wide variety of approaches encompassing both discrete units (e.g., agents, particles, information packages, viruses, goods or money) and continuous variables (e.g., electrical current, flows or influence). And (iii) heuristic approaches whose underlying generative dynamics are hidden, implicitly assumed or unknown. There are many such cases in the literature of network analysis, specially regarding the definition of centrality measures as we will illustrate next.

The aim of this perspective article was to expose that a hidden dynamical model lies at the origin of the common graph metrics; calling for a new point of view for graph analysis from the perspective of dynamical systems and to propose a generalised frame in which the generative model can be adapted to the needs of the real systems under study. Concerns regarding the lack of transparency,

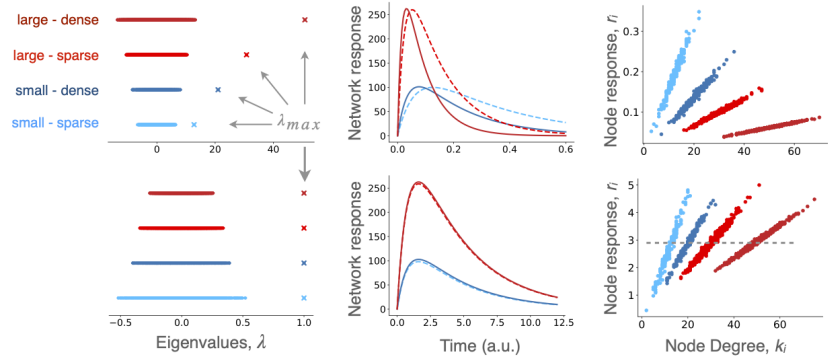
**A Comparison through null-models**



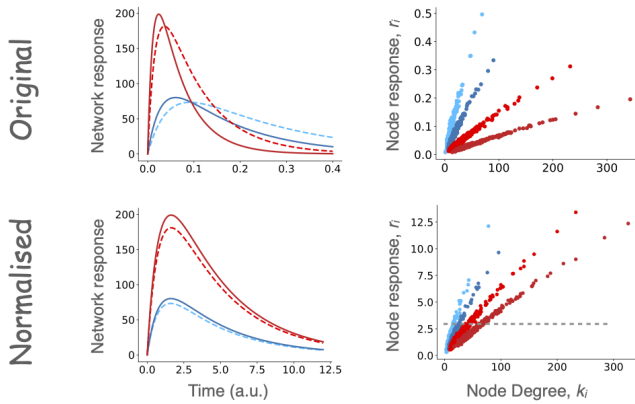
**B Network normalization**



**C Random graphs**



**D Scale-free-like**



**E Ring lattice**

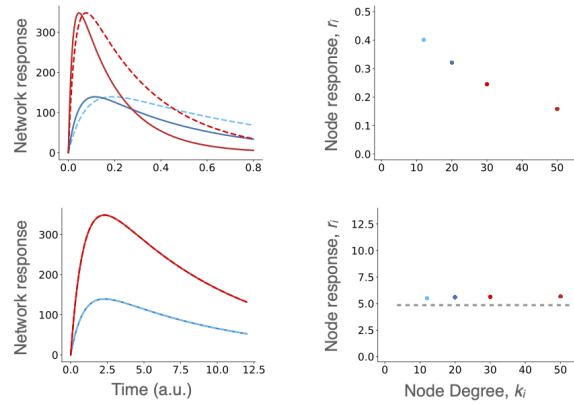


**FIG. 4. Normalising connectivity to compare networks.** **A** Schematic representation of classical approach in graph analysis to compare networks via third-party comparison to null-models. **B** Schematic representation of network comparison in the dynamical perspective. Normalising the connectivity matrices by their largest eigenvalues  $\lambda_{max}$  gives rise to weighted connectivities with aligned time-scales of evolution. **C – E** Testing network comparison by renormalisation of networks with largest eigenvalue for three familiar network models (random graphs of uniform probability, scale-free-like random graphs and ring lattices). Top panels display results out of the original (binary) adjacency matrices and bottom panels show results for the normalised connectivities. For each model, four distinct graphs were generated, from small and sparse to large and dense, combining sizes  $n_1 = 200$  nodes and  $n_2 = 500$  with densities  $\rho_1 = 0.06$  and  $\rho_2 = 0.1$ . Scale-free-like graphs were generated using degree-degree probabilities that would return an exponent  $\gamma = 3.0$  in the thermodynamical limit. The time-constant  $\tau$  for each network was set such that  $\tau = 0.8 \times \tau_{max}$ , where  $\tau_{max} = 1 / \lambda_{max}$ .

implicit assumptions and hidden generative dynamics is not new in the study of networks. Specially in respect of

definitions of centrality. The concept of centrality is intuitively related to propagation phenomena in networks. The literature has been prolific in proposing centrality measures, e.g. degree centrality, closeness centrality, betweenness centrality, eigenvector centrality and Katz centrality. The majority of those classic measures were defined following intuitive but *ad-hoc* rationale. The variety of centrality measures, the rather opaque definitions and the implicit assumptions behind them has led to debates calling for clarity<sup>30,31</sup>. As stated by S.P. Bogartti<sup>31</sup>:

What is not often recognized is that the formulas for these different measures make implicit assumptions about the manner in which things flow in a network (...) the discussion of centrality has largely avoided any mention of the dynamic processes that unfold along the links of a network (not to mention the processes that shape the network structure). Yet, the importance of a node in a network cannot be determined without reference to how traffic flows through the network.

And concludes that:

...the off-the-shelf formulas for centrality measures are fully applicable only for the specific flow processes they are designed for, and that when they are applied to other flow processes they get the ‘wrong’ answer. It is noted that the most commonly used centrality measures are not appropriate for most of the flows we are routinely interested in.

This conclusion very much resonates with the aim of this perspective, although here our aim is to generalise these ideas to the essence of graph analysis, beyond centrality measures.

To be fair, it shall be noted that in the recent years several centrality measures have been proposed for which the underlying propagation model is made explicit. For example, approaches based on propagation kernels tunable for various spatial scales<sup>32</sup>, the propagation of random walkers<sup>17,19</sup>, or a measure based on the conservative diffusion mediated by the Laplacian matrix<sup>24</sup>, i.e., the same system defined in Eq. (11). We now expose the *hidden* dynamical origin and the implicit assumptions of two popular network measures, a classic one (the Katz centrality) and a more recent one (communicability). We establish the connection between the two measures thanks to the dynamical viewpoint endorsed in this this article.

### Katz centrality and communicability

Given that the powers of the adjacency matrix  $(A^l)_{ij}$  determine the number of paths of length  $l$  between nodes, it has been often recognised in the literature that this construct should be key to explain the functional relation between two nodes, not only through the direct or

shortest paths, but encompassing all possible routes of any length to travel from node  $i$  to  $j$ . In fact, it has been often proposed that the influence of one node over another should depend on the accumulated routes that an agent could possibly travel between the two, say:

$$Q = A + A^2 + A^3 + A^4 + A^5 + \dots \quad (13)$$

The problem with this expression is that for any binary adjacency matrix the sum diverges as the values  $(A^l)_{ij}$  rapidly grow with length  $l$ . In order to avoid this, Katz (1952)<sup>33</sup> proposed to include an attenuation factor  $\alpha$  which “*has the force of a probability of effectiveness of a single link.*” In other words,  $\alpha$  is a weight given to the links in order to tune their efficiency of transmission. Then, the expression above is rewritten as follows:

$$Q^K = \alpha A + \alpha^2 A^2 + \alpha^3 A^3 + \alpha^4 A^4 + \alpha^5 A^5 + \dots \quad (14)$$

When  $\alpha < 1$  is small enough, this reduced efficiency of transmission should be able to compensate for the growth of the  $(A^l)_{ij}$  and guarantee the convergence of the sum. This is achieved for  $\alpha < 1/\lambda_{max}$ . Notice that  $\alpha A$  is now a weighted graph. The influence matrix  $Q^K$  can be reduced to:

$$Q = I + \alpha A + \alpha^2 A^2 + \dots = \sum_{l=0}^{\infty} (\alpha A)^l = \frac{1}{I - \alpha A}, \quad (15)$$

where  $I$  is the identity matrix. Following this, Katz defined a centrality of all nodes in the network  $\mathbf{C}^K$  as:

$$\mathbf{c}^K = \left( \frac{1}{I - \alpha A} - I \right) \mathbf{u} = Q^K \mathbf{u}, \quad (16)$$

where  $\mathbf{u}$  is the unit vector  $\mathbf{u}^T = (1, 1, \dots, 1)$  and the matrix  $Q^K$  encodes the net *influence* that one node exerts over another through all possible paths at all distances, given that at every step along the path influence decays by the ratio  $\alpha$ . Katz centrality  $c_i^K$  thus quantifies the summed influence that a unit perturbation applied to all nodes, the vector  $\mathbf{u}$ , has over node  $i$ —excluding the self-influence triggered by the perturbation  $u_i$  at node  $i$ . It is also common to find in the literature the Katz centrality expressed as  $\mathbf{c}^K = (I - \alpha A)^{-1} \mathbf{u}$  which includes the self-influence.

Another popular approach motivated to characterise the influence of nodes beyond shortest paths has been the communicability metric<sup>34</sup>. In this case, the solution to guarantee the convergence of the sum of the powers  $A^k$ , Eq. (14), was to choose the factorial coefficients  $1/l!$  such that

$$I + A + \frac{1}{2!}A^2 + \frac{1}{3!}A^3 + \dots = \sum_{l=0}^{\infty} \frac{A^l}{l!}. \quad (17)$$

This series converges for all positive definite matrices  $A$  as it is the series expansion of the matrix exponential  $e^A$ .

Optionally, a factor  $\alpha$  can be included to define communicability as the following pair-wise influence matrix:

$$Q^C = \mathbf{I} + \alpha A + \frac{1}{2!} \alpha^2 A^2 + \dots = \sum_{l=0}^{\infty} \frac{(\alpha A)^l}{l!} = e^{\alpha A}. \quad (18)$$

In both approaches, the factor  $\alpha$  tunes the “depth” at which influence can be exerted. When  $\alpha = 0$  no information or influence can pass across the links. Increasing  $\alpha$  will first favour transmission along direct connections and then the shorter paths. Increasing  $\alpha$  will eventually allow the longer paths to take effect and—for the case of the Katz centrality—when  $\alpha > 1/\lambda_{max}$  it will make the  $Q^K$  to diverge. The factor  $\alpha$  can be regarded either as an attenuation factor, a resistance or more generally, as a coupling strength associated to the links.

The rationale behind Katz centrality and communicability is identical as both approaches define a metric of pair-wise influence exerted over all possible paths, of all lengths. The only difference between the two approaches is that Katz centrality assumes a constant tuning or attenuation of all paths, regardless of their length. That is, at every step, the propagation through a link suffers the same attenuation  $\alpha$ , regardless of how many steps were given before. In contrast, the nonlinear factorial coefficients  $\frac{1}{l!}$  of communicability punish the longer paths in excess, which enforces the convergence.

In other words, the only difference between Katz centrality and communicability is that they are the result of a different propagation model. It is rather trivial to show that Katz centrality is driven by the leaky-cascade of Eq. (7) while communicability is the product of the continuous cascade in Eq. (4). Given the leaky cascade subjected to a constant input  $\mathbf{1}$ ,  $\dot{\mathbf{x}} = -\mathbf{x}/\tau + A\mathbf{x} + \mathbf{1}$ , the steady-state solution ( $\dot{\mathbf{x}} = \mathbf{0}$ ) is given by  $(\mathbf{I}/\tau - A)\tilde{\mathbf{x}} = \mathbf{1}$ . Solving for  $\tilde{\mathbf{x}}$  we have that<sup>35–38</sup>:

$$\tilde{\mathbf{x}} = \left( \frac{1}{\mathbf{I}/\tau - A} \right) \mathbf{1}, \quad (19)$$

which is, precisely the definition of Katz centrality ( $\tilde{\mathbf{x}} \equiv \mathbf{c}^K$ ) in the version that accounts for the self-influences and with the attenuation factor being  $\alpha = \tau$ . Whether  $\alpha$  divides the self activity of the nodes (the term  $-\mathbf{x}/\alpha$ ) or multiplies the connectivity matrix ( $\alpha A$ ), and whether it is interpreted as a dissipation factor, a leakage term, a coupling strength or an attenuation factor, this is just a matter of convenience to be coherent with the real system under study. Mathematically, those forms are all identical.

Now, recalling that the solution of the continuous cascade  $\dot{\mathbf{x}}(t) = A\mathbf{x}(t)$  to initial conditions  $\mathbf{x}_0$  is given by  $\mathbf{x}(t) = e^{At} \mathbf{x}_0$ , it becomes clear that communicability is just the propagator—the Green function—of the discrete cascade:

$$Q^C \equiv e^{At} = \mathbf{I} + At + \frac{1}{2!} (At)^2 + \dots = \sum_{l=0}^{\infty} \frac{(At)^l}{l!}. \quad (20)$$

This expression clarifies the intrinsic relation between the “attenuation factor”  $\alpha$  and the depth of the paths involved in the influence between nodes. After a short time  $t > 0$ , transmission along the shorter paths dominates but as time passes the influence of the longer paths starts to take effect. This is reflected in the evolution of the response matrices for the continuous cascade in Fig. 2B. The initial response matrix very much resembles the adjacency matrix, since the accumulated influence is dominated by the direct connections but, as time passes, the influence through the longer paths takes effect; leading to a pair-wise response architecture that is dissociated from  $A$  and only the degrees of the nodes matter. Also, the origin of the communicability on the continuous cascade exposes that communicability is divergent by definition and hence, analysis of communicability—same as for the standard graph metrics—shall be bounded to the shorter time-scales with a temporal cut-off. This could be somehow alleviated by adding the attenuation constant or a coupling strength to the system,  $\dot{\mathbf{x}}(t) = \alpha A \mathbf{x}(t)$ , in order to tune rate of divergence of communicability as  $Q^C = e^{\alpha A t}$ .

We cannot close this brief overview without mentioning the extensive efforts done in the recent years to define network metrics for the case of random walkers. Given their Markovian and conservative nature, processes of random walkers on networks are mathematically tractable and well-behaved (the dynamics do not diverge). Hence, random walkers represent a convenient approach to explore networks and to define metrics to characterise them, much in the line of the goals of the present article. Besides the aforementioned centrality measures, significant work has been done to identify communities based on the susceptibility of a walker to remain trapped in a module or to jump from one community to another<sup>17,19,39</sup>.

## VI. DISCUSSION

Traditionally, graph theory has been considered as a data-driven analysis tool and therefore, its metrics applicable to any system that is represented as a graph. Methods to explore and characterise networks based on propagation processes have also been proposed, specially regarding the definition of centrality measures and community detection. Sometimes, those methods have been defined following *ad-hoc* rationale, e.g., Katz centrality and communicability; based on the idea that the powers of the adjacency matrix inform of the number of non-Hamiltonian paths from one node to another, instead of being derived from first principles. Other efforts have explicitly employed processes of random walkers to define diverse methods, e.g., to identify communities. In any case, whether the underlying dynamics were implicit or explicit, all those methods have been proposed as if they were universal, useful to study any network.

Here, we have exposed that classical graph metrics (e.g., degree, matching index, clustering coefficient and geodesic distance) are founded on a hidden generative propagation model: the discrete cascade. We have also shown that other network metrics—the Katz centrality and the communicability—which are usually thought as generic or model agnostic metrics, are also the product of specific propagation models. Communicability originates from the continuous cascade in Eq. (4), and Katz centrality is derived from the continuous leaky cascade in Eq. (7). These observations reveal that, contrary to the common belief, graph analysis is not data-driven but model based.

Now, the problem with model-based data analysis methods is that of model selection. In statistics for example, one would never apply certain metrics to a dataset unless the data passes a Gaussianity test before. Because if the dataset were not Gaussian, the outcome of those measures would not be interpretable. So, graph analysis needs its particular Gaussianity test. We advocate for transparent network analysis tools in which the underlying dynamical model, the assumptions and the constraints are explicit, instead of hidden or implicitly defined. And, we will have to recognise that graph metrics are not universal. All graph metrics are valid. The traditional metrics (clustering, geodesic distance, etc.), Katz centrality, communicability, community detection based on random walkers, and so on. All those all are valid formulations to characterise graphs and complex networks. The question is not whether they are useful, but to understand *when and where* is meaningful to use them.

Once we have acknowledged that graph analysis is a model-based data analysis tool, we are free to replace the underlying propagation model and design analyses that are better suited for particular real networks. We imagine that in the future, before performing a network analysis, a user will first identify which are the fundamental constraints of the real system investigated. Is it discrete, or is it a continuous system? Is it conservative or non-conservative? Once the fundamental ingredients of the system are clear, the user will select the right model that satisfies those conditions and develop a personalised network analysis that is tuned for that real network; or for a family of real networks.

For this scenario to be plausible, the remaining challenge is to define those model-based measures for different propagation models. Here, we have proposed a possibility inspired by the fact that the typical graph metrics can be derived as spatio-temporal properties of the network responses to a unit perturbation. Our proposal is to derive the network (pair-wise) response function  $\mathcal{R}(t)$  (i.e., the Green function of the network for a given propagation model), and to extract the information about the network from the corresponding  $\mathcal{R}(t)$ . Although defining such network metrics might not always be trivial, we have shown that this dynamical point of view to network analysis brings several benefits. First, we could illustrate that, in fact, networks look different seen through the

lense of different propagation models. Even for the same network, each model highlights some aspects of the network and ignores others. Second, this approach can naturally deal with weighted networks—as long as the meaning of the weights is compatible with the dynamical process. And third, normalizing the connection weights of networks by their largest eigenvalues, aligns their temporal scales facilitating their comparison without the need of using null-models.

We conclude with the following reflection. Given the number of existing centrality measures, how comes that PageRank became so successful? Very likely, the answer is simply that the propagation model behind PageRank is a crude but a reasonable approximation to the underlying human behaviour while navigating the internet. The implicit assumptions and propagation models behind other centrality measures were not compatible with the description of humans surfing the world-wide web. We believe that if network analysis as a field overcomes the idea of graph theory and its satellite approaches as being universal tools that serve for all networks, if the field transitions into more personalised analysis strategies that transparently and naturally encompasses the minimal constraints and assumptions of each real system, we will see other success stories similar to that of PageRank. We understand that such a transition can only happen at the cost of universality—a price many will find difficult to pay—but by doing so there is plenty of specificity and interpretability to gain. With this in mind, we shall stress that the dynamical perspective we have discussed here, while it serves as an umbrella to encompass many of the existing analyses and approaches, it is neither to be regarded as *the ultimate* solution. Surely there are many real-world systems susceptible of a network representation but whose analysis in terms of propagation and navigation is not suitable. Their study may require employing other forms of network analyses. In this new scenario that is opening, what matters is to choose the right tools for right case.

## ACKNOWLEDGMENTS

This work has been supported (GZL and MG) by the European Union’s Horizon 2020 research and innovation programme under Specific Grant Agreement No. 785907 (HBP SGA2) and Specific Grant Agreement No. 945539 (Human Brain Project SGA3). MG also acknowledges funding from the Marie Skłodowska-Curie Action (Grant H2020-MSCA-656547) of the European Commission.

### Appendix: Dynamical representation of graph metrics

From the point of view of graph theory, all the relevant information about the network is encoded in the adjacency matrix  $A$ . Combinatorial or algorithmic methods allow then to answer different questions about the architecture of the graph in the form of graph metrics. The dynamical paradigm shown in the previous sections exposes that under the discrete cascade in Eq. (1), the structural information in  $A$  is unfolded into the set of powers  $\mathcal{R} = \{A^0, A^1, A^2, A^3, \dots, A^t\}$  representing the temporal response of the network to an initial perturbation in all nodes. We now show how fundamental graph metrics are encoded by the response matrices  $\mathcal{R}$ .

The *degree* of a node,  $k$ , is defined as the number of neighbours of the node. Usually, it is calculated as the row or column sum of the adjacency matrix such that  $k_i = \sum_{j=1}^n A_{ij}$ . In the dynamical perspective, the degree is expressed as the number of particles returning to the node in the short time scales. A particle starting at node  $i$  produces that each neighbour of  $i$  receives one particle in the first iteration. In the second iteration,  $t = 2$ , new particles will propagate to the neighbours of each node. The single particle starting from  $i$  at  $t = 0$  results in  $i$  receiving one particle per neighbour at time  $t = 2$ . In other words, the degree is the influence that a node exerts on itself at time  $t = 2$  and it is thus represented by the diagonal elements of  $A^2$ :

$$k_i = (A^2)_{ii}. \quad (\text{A.1})$$

*Matching index* is a measure of the structural similarity between two nodes. It is evaluated counting the number of common neighbours since, two nodes that share the same connections play an identical role in the graph. Given that  $\mathcal{N}(v)$  is the set of nodes connected to vertex  $v$ —the neighbourhood of  $v$ —the number of common neighbours between two nodes is quantified as the size of the overlap of their neighbourhoods:  $m(i, j) = |\mathcal{N}(i) \cap \mathcal{N}(j)|$ . From the adjacency matrix  $m(i, j)$  is calculated comparing the rows corresponding to the two nodes such that  $m(i, j) = \sum_{k=1}^n A_{ik}A_{jk}$ . Usually, the matching index  $M(i, j)$  is normalised by the fraction between the number of common neighbours and the total number of nodes adjacent to either  $i$  or  $j$ :

$$M(i, j) = \frac{|\mathcal{N}(i) \cap \mathcal{N}(j)|}{|\mathcal{N}(i) \cup \mathcal{N}(j)|} = \frac{m(i, j)}{k_i + k_j - m(i, j)}. \quad (\text{A.2})$$

Thus,  $M(i, j) = 0$  when  $i$  and  $j$  have no neighbours in common and  $M(i, j) = 1$  when both nodes are connected to the same, and only the same, neighbours.

Under the perspective of the discrete cascading, the overlap  $m(i, j)$  can be regarded as the “convergence zone” of two simultaneous propagations, one starting from  $i$  and the other from  $j$ . Imagine the initial conditions  $\mathbf{x}_0$  with  $x_{k,0} = 1$  if  $k = i, j$  and  $x_{k,0} = 0$  otherwise. After the first iteration nodes adjacent to either  $i$  or  $j$  will receive one particle and the only nodes with two particles are

those adjacent to both  $i$  and  $j$ . At the second time-step, node  $j$  receives one particle, due to the initial one on  $i$  at  $t = 0$ , from each of the nodes shared with  $i$ . Therefore, the number of common neighbours  $m(i, j)$  between  $i$  and  $j$  is reflected in the matrix element  $(A^2)_{ij}$ . In other words, the influence that  $i$  exerts on  $j$  at time  $t = 2$ —or the influence of  $j$  on  $i$ —is mediated exclusively via their common neighbours. If they had no common neighbours, then there is no influence between them at this time step. As shown before, the degrees  $k_i$  are encoded in the entries  $(A^2)_{ii}$ , thus substituting in Eq. (A.2) we can express the matching index in terms of the discrete propagation as:

$$M(i, j) = \frac{(A^2)_{ij}}{(A^2)_{ii} + (A^2)_{jj} - (A^2)_{ij}}, \quad (\text{A.3})$$

This expression illustrates that in dynamical terms the normalised matching index is regarded as the fraction of the influence between two nodes that is routed via the common neighbours, and it thus invites for a generalization of the index to subsequent time steps  $t > 2$  by allowing the subsequent powers into Eq. (A.3). Such a generalisation should also open the door to define an equivalent metric when the underlying discrete cascade is replaced by other more general dynamical models.

The *clustering coefficient*,  $C$ , is a popular graph metric. It quantifies the probability that the neighbours of one node are connected with each other. In social terms, it answers the question of how likely is that “my friends are also friends with each other”. In practice, the clustering coefficient is calculated by counting the number of triangles in a graph since a link between two neighbours of a node leads to a triangle. It is well-known that the diagonal entries of  $A^3$  represent the number of triangles—cycles of length  $l = 3$ —in which nodes participate and that the total number of triangles in a graph is given by  $n(\triangle) = \frac{1}{3} \text{tr}(A^3) = \frac{1}{3} \sum_{i=1}^n (A^3)_{ii}$ , where the factor  $\frac{1}{3}$  is to account for the fact that every triangle is counted once per node. For the clustering coefficient to be a probability, it is normalised by the total number of triads  $n(\vee)$ , or paths of length  $l = 2$  in the graph. Thus,  $C$  is 1 only if all the triads form closed paths. In terms of the powers of  $A$ , the total number of paths of length  $l = 2$  is calculated as  $n(\vee) = |A^2| - \text{tr}(A^2)$ , where  $|\cdot|$  represents the sum of all the elements of the matrix, and  $\text{tr}(\cdot)$  is the trace. So, the clustering coefficient is calculated as:

$$C = 3 \frac{n(\triangle)}{n(\vee)} = \frac{\text{tr}(A^3)}{|A^2| - \text{tr}(A^2)}. \quad (\text{A.4})$$

Under the dynamical perspective of the discrete cascading in Eq. (1), the quantity  $|A^2| - \text{tr}(A^2)$  represents the number of particles that are generated in the iteration from  $t = 1$  to  $t = 2$ , or in other words, the total influence exerted across nodes at time  $t = 2$ . The quantity  $\text{tr}(A^3)$  is the number of particles returning to the nodes, or the self-influence at  $t = 3$ . Thus, in dynamical terms the clustering coefficient can be interpreted as how much of the influence generated by the network at time  $t = 2$  falls back to the nodes at  $t = 3$ .

It shall be noted that if the degree is a metric of the influence of a node over itself at  $t = 2$ , the clustering coefficient is a metric of the influence that nodes exert on themselves at time  $t = 3$ . The difference is that the clustering is normalised in order to take the form of a probability. Last, the dynamical definition of  $C$  allows for a natural generalisation of the probability of self-interaction at any time, such that for all  $t > 1$ ,

$$C_t = \frac{\text{tr}(A^t)}{|A^{t-1}| - \text{tr}(A^{t-1})}. \quad (\text{A.5})$$

The *distance*,  $d_{ij}$ , between two nodes in a graph is defined as the minimal number of links needed to traverse in order to reach  $j$  from  $i$ . Graph distance cannot be derived from the adjacency matrix alone. Its calculation requires to navigate through the graph, e.g. based upon DFS or BFS algorithms. As mentioned before, the cascading process described in Eq. (1) is indeed the BFS navigation without memory. Under this cascading, instead of counting the number of jumps to travel between nodes,  $d_{ij}$  can be evaluated in terms time; the time needed for a cascade initialised at node  $i$  to first reach node  $j$ . That is, in dynamical terms graph distance can be regarded as the time a perturbation on a node needs to reach the rest of nodes. Given the set of matrix powers  $\mathcal{R} = \{A^0, A^1, A^2, A^3, \dots, A^t\}$ , we can formally redefine graph distance as:

$$d_{ij} = t' : (A^{t'})_{ij} > 0 \text{ if for all } t < t', (A^t)_{ij} = 0. \quad (\text{A.6})$$

Our overall goal is to generalise graph analysis by replacing the original generative dynamical model behind graph metrics, Eq. (1), with other models which account for other basic properties of real systems. The interpretation of distance in terms of the time required for perturbations to propagate will become a handful change of perspective under arbitrary dynamical rules, either discrete or continuous as we will derive in the following sections.

## REFERENCES

- <sup>1</sup>Stephen P Borgatti, Ajay Mehra, Daniel J Brass, and Giuseppe Labianca. Network analysis in the social sciences. *Science*, 323:892–895, 2009.
- <sup>2</sup>I. Kiss, J. C. Miller, and P. L. Simon. *Mathematics of epidemics on networks*, volume 46 of *Interdisciplinary applied mathematics*. Springer, 2017.
- <sup>3</sup>M. Kaiser. Brain architecture: a design for natural computation. *Phil. Trans. R. Soc. A*, 365:3033–3045, 2007.
- <sup>4</sup>G. Zamora-López, C. S. Zhou, and J. Kurths. Exploring brain function from anatomical connectivity. *Front. Neurosci.*, 5:83, 2011.
- <sup>5</sup>A. Baronchelli, R. Ferrer i Cancho, R. Pastor-Satorras, N. Chater, and M. H. Christiansen. Networks in cognitive science. *Trends Cogn. Sci.*, 17(7):348–360, 2013.
- <sup>6</sup>D. Papo, M. Zanin, J.A. Pineda-Pardo, S. Boccaletti, and J.M. Buldú. Functional brain networks: great expectations, hard times and the big leap forward. *Phil. Trans. R. Soc. B*, 369:20130525, 2014.
- <sup>7</sup>H Jeong, B Tombor, R Albert, Z N Oltvai, and A L Barabási. The large-scale organization of metabolic networks. *Nature*, 407:651–654, 2000.
- <sup>8</sup>B. H. Junker and F. Schreiber, editors. *Analysis of biological networks*. Wiley-interscience, Hoboken, New Jersey, USA, 2008.
- <sup>9</sup>M. Wickramasinghe and I.Z. Kiss. Spatially organized dynamical states in chemical oscillator networks: Synchronization, dynamical differentiation, and chimera patterns. *PLoS ONE*, 8(11):1862–1867, 2013.
- <sup>10</sup>C. Bick, M. Sebek, and I.Z. Kiss. Robust weak chimeras in oscillator networks with delayed linear and quadratic interactions. *Phys. Rev. Lett.*, 119:168301, 2017.
- <sup>11</sup>Andrei Broder, Ravi Kumar, Farzin Maghoul, Prabhakar Raghavan, Sridhar Rajagopalan, Raymie Stata, Andrew Tomkins, and Janet Wiener. Graph structure in the web. *Comput Netw*, 33:309–320, 2000.
- <sup>12</sup>A. Arenas, A. Díaz-Guilera, J. Kurths, Y. Moreno, and C. Zhou. Synchronization in complex networks. *Phys. Repts.*, 469:93–153, 2008.
- <sup>13</sup>A. Barrat, M. Barthélemy, and A. Vespignani. *Dynamical processes on complex networks*. Cambridge University Press, 2008.
- <sup>14</sup>N. Masuda, M. A. Porter, and R. Lambiotte. Random walks and diffusion on networks. *Phys. Repts.*, 716(717):1–58, 2017.
- <sup>15</sup>P. Ji, J. Ye, Y. Mu, W. Lin, Y. Tian, C. Hens, M. Perc, Y. Tang, J. Sun, and J. Kurths. Signal propagation in complex networks. *Phys. Repts.*, 1017:1–96, 2023.
- <sup>16</sup>S.-J. Yang. Exploring complex networks by walking on them. *Phys Rev. E*, 71:016107, 2005.
- <sup>17</sup>M. Rosvall and C. T. Bergstrom. Maps of random walks on complex networks reveal community structure. *Proc. Nat. Acad. Sci.*, 105(4):1118–1123, 2008.
- <sup>18</sup>M. Bogu ná, D. Krioukov, and K. C. Claffy. Navigability of complex networks. *Nat. Physics*, 5:74–80, 2009.
- <sup>19</sup>J.-C. Delvenne, S. N. Yaliraki, and M. Barahona. Stability of graph communities across time scales. *Proc. Nat. Acad. Sci.*, 107(29):12755–12760, 2010.
- <sup>20</sup>M. Gilson, N.-E. Kouvaris, G. Deco, and G. Zamora-López. Framework based on communicability and flow to analyze complex network dynamics. *Phys. Rev. E*, 97:052301, 2018.
- <sup>21</sup>M. Gilson, N. E. Kouvaris, G. Deco, J.-F. Mangin, C. Poupon, S. Lefranc, D. Rivière, and G. Zamora-López. Network analysis of whole-brain fmri dynamics: A new framework based on dynamic communicability. *NeuroImage*, 201:116007, 2019.
- <sup>22</sup>G. Zamora-López and R. Brasselet. Sizing complex networks. *Comms. Phys.*, 2:144, 2019.
- <sup>23</sup>G. Zamora-López, C. S. Zhou, and J. Kurths. Cortical hubs form a module for multisensory integration on top of the hierarchy of cortical networks. *Front. Neuroinform.*, 4:1, 2010.
- <sup>24</sup>A. Arnaudon, R. L. Peach, and M. Barahona. Scale-dependent measure of network centrality from diffusion dynamics. *Phys. Rev. Research*, 2:033104, 2020.
- <sup>25</sup>A. Arenas, A. Díaz-Guilera, and C. Pérez-Vicente. Synchronization reveals topological scales in complex networks. *Phys. Rev. Lett.*, 96:114102, 2006.
- <sup>26</sup>A. Bovet, J.-C. Delvenne, and R. Lambiotte. Flow stability for dynamic community detection. *Sci. Adv.*, 8:eabj3063, 2022.
- <sup>27</sup>X. Wu, C.S. Zhou, G. Chen, and J.-A. Lu. Detecting the topologies of complex networks with stochastic perturbations. *Chaos*, 21:043129, 2011.
- <sup>28</sup>E. Bianco-Martinez, N. Rubido, C. G. Antonopoulos, and M. S. Baptista. Successful network inference from time-series data using mutual information rate. *Chaos*, 26:043102, 2016.
- <sup>29</sup>M. Asllani, B.R. Da Cunha, E. Estrada, and J. P. Gleeson. Dynamics impose limits to detectability of network structure. *New J. Phys.*, 22:063037, 2020.
- <sup>30</sup>N. E. Friedkin. Theoretical foundations for centrality measures. *Am. J. Sociol.*, 96:1478–1504, 1991.
- <sup>31</sup>S. P. Bogartti. Centrality and network flow. *Social Networks*, 27:55–71, 2005.
- <sup>32</sup>J. Zhang, X.-K. Xu, P. Li, K. Zhang, and M. Small. Node im-



- portance for dynamical process on networks: A multiscale characterization. *Chaos*, 21:016107, 2011.
- <sup>33</sup>L. Katz. A new status index derived from sociometric analysis. *Psychometrika*, 18(1):39–43, 1952.
- <sup>34</sup>E. Estrada and N. Hatano. Communicability in complex networks. *Phys Rev. E*, 77:036111, 2008.
- <sup>35</sup>G. Tononi, O. Sporns, and G. M. Edelman. A measure for brain complexity: relating functional segregation and integration in the nervous system. *Proc. Nat. Acad. Sci.*, 91:5033–5037, 1994.
- <sup>36</sup>R.F. Galán. On how network architecture determines the dominant patterns of spontaneous neural activity. *PLoS ONE*, 3(5):e2148, 2008.
- <sup>37</sup>G. Zamora-López, Y. Chen, G. Deco, M. L. Kringelbach, and C. S. Zhou. Functional complexity emerging from anatomical constraints in the brain: the significance of network modularity and rich-clubs. *Sci. Reps.*, 6:38424, 2016.
- <sup>38</sup>K. J. Sharkey. A control analysis on katz centrality. *Sci. Reps.*, 7:17247, 2017.
- <sup>39</sup>M.T. Schaub, R. Lambiotte, and M. Barahona. Encoding dynamics for multiscale community detection: Markov time sweeping for the map equation. *Phys Rev. E*, 86:026112, 2012.